



Article

Quantification of Fluid Volume and Distribution in the Paediatric Colon via Magnetic Resonance Imaging

Jan Goelen¹, Benoni Alexander², Haren Eranga Wijesinghe³, Emily Evans³, Gopal Pawar¹ , Richard D. Horniblow² and Hannah K. Batchelor^{4,*}

¹ School of Pharmacy, Institute of Clinical Science, University of Birmingham, Edgbaston, Birmingham B15 2TT, UK; JXG918@student.bham.ac.uk (J.G.); G.Pawar@bham.ac.uk (G.P.)

² School of Biomedical Science, Institute of Clinical Science, University of Birmingham, Edgbaston, Birmingham B15 2TT, UK; benoni.alexander@gmail.com (B.A.); R.Horniblow@bham.ac.uk (R.D.H.)

³ Department of Radiology, University Hospital Coventry & Warwickshire, Clifford Bridge Road, Coventry CV2 2DX, UK; haren_wijesinghe@hotmail.com (H.E.W.); emilylivesey58@gmail.com (E.E.)

⁴ Strathclyde Institute of Pharmacy and Biomedical Sciences, University of Strathclyde, Glasgow G4 0RE, UK

* Correspondence: hannah.batchelor@strath.ac.uk; Tel.: +44-141-548-2125

Abstract: Previous studies have used magnetic resonance imaging (MRI) to quantify the fluid in the stomach and small intestine of children, and the stomach, small intestine and colon of adults. This is the first study to quantify fluid volumes and distribution using MRI in the paediatric colon. MRI datasets from 28 fasted (aged 0–15 years) and 18 fluid-fed (aged 10–16 years) paediatric participants were acquired during routine clinical care. A series of 2D- and 3D-based software protocols were used to measure colonic fluid volume and localisation. The paediatric colon contained a mean volume of 22.5 mL ± 41.3 mL fluid, (range 0–167.5 mL, median volume 0.80 mL) in 15.5 ± 17.5 discreet fluid pockets (median 12). The proportion of the fluid pockets larger than 1 mL was 9.6%, which contributed to 94.5% of the total fluid volume observed. No correlation was detected between all-ages and colonic fluid volume, nor was a difference in colonic fluid volumes observed based on sex, fed state or age group based on ICH-classifications. This study quantified fluid volumes within the paediatric colon, and these data will aid and accelerate the development of biorelevant tools to progress paediatric drug development for colon-targeting formulations.

Keywords: intestinal fluid; MRI; paediatrics; biorelevant dissolution; large bowel; colon



Citation: Goelen, J.; Alexander, B.; Wijesinghe, H.E.; Evans, E.; Pawar, G.; Horniblow, R.D.; Batchelor, H.K.

Quantification of Fluid Volume and Distribution in the Paediatric Colon via Magnetic Resonance Imaging.

Pharmaceutics **2021**, *13*, 1729.

<https://doi.org/10.3390/pharmaceutics13101729>

Academic Editors: Charles M. Heard

Received: 8 September 2021

Accepted: 14 October 2021

Published: 19 October 2021

Publisher's Note: MDPI stays neutral with regard to jurisdictional claims in published maps and institutional affiliations.



Copyright: © 2021 by the authors. Licensee MDPI, Basel, Switzerland. This article is an open access article distributed under the terms and conditions of the Creative Commons Attribution (CC BY) license (<https://creativecommons.org/licenses/by/4.0/>).

1. Introduction

Oral drugs are the most common form of drug administration due to both patient convenience and the favourable cost:benefit ratio [1,2]. Despite the clear advantages of oral formulations, such preparations rely on drug liberation and dissolution for absorption. The free water available at the site of dissolution is a critical parameter for these processes as it also affects local drug concentration and thus permeation [3–5]. As such, a comprehensive understanding of the amount and distribution of fluid throughout the gastrointestinal tract (GIT) is required to ensure appropriate and adequate absorption of oral medicines [6]. This is important for colon-targeted formulations, which have gained increased interest from the pharmaceutical industry [7–9], for local action or systemic absorption [10–12]. Increasing the absorption window of a drug by targeting the colon offers advantages in terms of frequency of dosing, where controlled or extended release (XR) formulations can be used to enable once daily dosing (improving patient convenience [8], maintaining therapeutic concentrations [13] and reducing the risk of administration errors [14]). The low proteolytic activity and the potential of intact peptide absorption [15] (as demonstrated for insulin [16] or linaclotide [17]) enables the large intestine (with emphasis on the proximal colon) as an appropriate absorption site [5,18].

Colon-targeting formulations are often designed to exploit local intestinal environment characteristics for drug release, such as pH or the presence of bacterial-derived

metabolising enzymes [10,12]. Although some XR-formulations are designed to deliver drugs independent of local environmental factors (such as time-dependent release, such as mesalazine preparations for ulcerative colitis treatment [19]), the performance of these formulations needs to be evaluated in biorelevant conditions that include the colonic macroenvironment in terms of fluid volume and composition [14,20–22]. In addition, the influence of colonic fluid volumes on incomplete dissolution and absorption of poorly soluble drugs in the upper GIT and subsequent accumulation of solid drug particulates in the colon [23,24] (such as NSAIDs for treatment of colorectal cancer) is not fully understood.

Data on intestinal fluid (amount, distribution and composition) are necessary for in vitro and in silico models in drug development [3,5,8,11,14,25,26]. Despite recent efforts, there is no consensus on the volume of water or its distribution throughout the colon of adults [27], which translates in poor estimations for the standardised volume employed for colonic dissolution testing (Table 1). Currently, in vitro and in silico models of the colon use a range of volumes for dissolution assays, ranging from 1 mL to 200 mL [28–30].

Table 1. Reported fluid volumes in the colon of healthy adults when measured using MRI. N/A means that the data were not reported.

Study	Feed Status (Intake of Food/Fluid)	Time of Ingestion before MRI Acquisition	Number of Participants	Median (Min-Max) (mL)	Mean (\pm SD) (mL)
Schiller 2005 [31]	Fasted	-	12	8 (1–44)	13 \pm 12
	Fed (standardised meal)	1 h		18 (2–97)	11 \pm 26
Pritchard 2017 [32]	Fasted	-	11	2 (0–7)	-
	Fed (500 mL Moviprep)	1 h		140 (104–347)	-
Murray 2017 [3]	Fasted	-	12	N/A (0–11)	2 \pm 1
	Fed (240 mL water)	30 min		N/A (0–49)	7 \pm 4

As XR-formulations are associated with high inter-individual variability in vivo [33,34], it is recognised that prediction of performance of these products is challenging. The uncertainty is even more pronounced for paediatric XR-formulations, as the variability is increased due to the lack of physiologically relevant input data for in vitro and in silico models [2,35].

There is a recognised knowledge gap about the amount and distribution of free fluid in the GIT of the paediatric population [36–38], resulting in a need to generate physiological data to underpin the development of age appropriate physiologically based pharmacokinetic (PBPK) models. This would improve prediction of drug performance in children, as paediatric clinical trials often face ethical constraints [1,2]. No studies to date have quantified the amount and distribution of fluid in the paediatric colon [36–39], thus predictions of performance are based on extrapolation of adult data. Direct extrapolation of the adult values to the paediatric population is less appropriate, due to the reported differences in the paediatric anatomy and physiology of the GIT [1,40,41].

The free fluid in the GIT can be quantified by magnetic resonance imaging (MRI), a non-invasive tool that permits undisturbed visualisation of the GIT [7]. In contrast with scintigraphy or computed tomography (CT), no ionising radiation dose is needed for imaging [27] and its effectiveness in producing qualitative images enabling fluid quantification has been demonstrated [3,27,31,32,42,43].

Therefore, the aim of this study was to use MRI to locate and quantify the fluid volumes and number of pockets in the colon of a paediatric population.

2. Materials and Methods

2.1. Study Design and Participants

Our research group has access to an MRI databank showing the abdomen of 49 paediatric participants, which was used previously to quantify the volume of free fluid in the stomach and small intestine. This observational, retrospective study used the same MRI datasets to quantify the volume of free fluid in the colon (Ethical approval: REC reference: 18/EM/0251 (IRAS 237159 MRI: Fluid volumes and localisation in paediatric GI tract)). Following exclusion criteria were applied to ensure the cohort was as healthy as possible: patients with acute abdomen (appendicitis or perforated viscus), malignant bowel disease, surgery (bowel section, excluding appendectomy), bowel wall thickening/stricture/fistula/abscess. The datasets originated from two sites: Birmingham Children's Hospital (BCH) and University Hospitals Coventry and Warwickshire NHS Trust (UHCW). All participants were fasted overnight and in addition, the UHCW site required the children to ingest 500 mL of Oral Klean Prep (a macrogol-based osmotic laxative) 60 min before MRI acquisition. This enabled the study to include a fasted and a fluid-fed population. The MRI acquisition parameters are listed in Table 2.

Table 2. MRI scanner and acquisition parameters.

Site	UHCW	UHCW	BCH	BCH
Participants	Fluid-fed	Fluid-fed	Fasted	Fasted
1.5 T MR Imaging Unit: series and manufacturer	Optima MR450w, GE Healthcare, Chicago, IL, USA	Aera, Siemens Healthcare, Erlangen, Germany	Siemens MAGNETOM Avanto 1.5 T MRI System, Siemens Healthcare, Erlangen, Germany	Aera, Siemens Healthcare, Erlangen, Germany
MRI coil	48-channel body coil	body coil	16-element parallel imaging receiver coil	16-element parallel imaging receiver coil
MRI protocol	Coronal balanced steady-state gradient echo sequence (fast-imaging employing steady-state acquisition, FIESTA)	Coronal balanced steady-state gradient echo sequence (true FISP)	Coronal T2 SPACE sequence	Coronal T2 SPACE sequence
Median slice thickness (range)	4.0 mm (2.998 mm–6 mm)	6.0 mm (2.998 mm–6 mm)	0.9 mm (0.09 mm–0.55 mm)	0.9 mm (0.09 mm–0.55 mm)
Echo train length	1	1	1	1
Median intersection gap	5.0 mm	3.0 mm	None	None
Matrix	0.35 × 0.35 mm	1.0 × 1.0 mm	0.8 × 0.8 mm	0.8 × 0.8 mm
Field of view	420 cm ²	420 cm ²	250 cm ²	400 cm ²
TR/TE	5.7/1.9 ms	652.8/2.1 ms	1700/98 ms	2000/241 ms

2.2. Data Processing

Only datasets with good resolution and correct T2-weighted MRI sequence were included in the study; this was a total of 46 MRI acquisitions. A 2D- and 3D-model were used to quantify the fluid within the MRI datasets.

2.2.1. D-Protocol

Two software packages were used for the 2D-fluid volume determination (Figure 1):

1. Horos [44] to identify and highlight the fluid pockets in the MRI dataset;
2. ImageJ to calculate the area of the marked fluid regions.

Horos is an open-source code software program distributed free of charge under the LGPL license at Horosproject.org and sponsored by Nimble Co LLC d/b/a Purview in Annapolis, MD, USA. Fluid identification within the MRI slices was based on the intensity of cerebrospinal fluid (CSF) which is routine in interpretation of these images [3,4,31,42,45]. The average voxel intensity within the CSF was used as threshold value for free fluid. The plug-in Global Thresholding Tool [46] then identified and highlighted all zones in the entire MRI dataset with a voxel intensity equal or higher than the threshold value (thus representing free fluid) in red (Figure 1B). These marked images were transferred to ImageJ [47], where the two dimensional area of the highlighted zones were calculated (Figure 1C,D). The volume of each zone was calculated by multiplying the highlighted area by the sum of the slice thickness and the interstitial slice gap. The volume, number and location of the fluid pockets were recorded for every participant. The location (ascending, transverse or descending colon) of fluid pockets were manually determined [48]. Paediatric radiologists assisted in defining the pocket's location. The first image slice (when migrating dorsal to ventral) showing the hepatic flexure is where the transverse colon was determined to start (on both the ascending-transversal and transversal-descending junctions). This enabled the exclusion of areas that were motion artefacts [49]. A sub-set of 20% were analysed by a second operator.

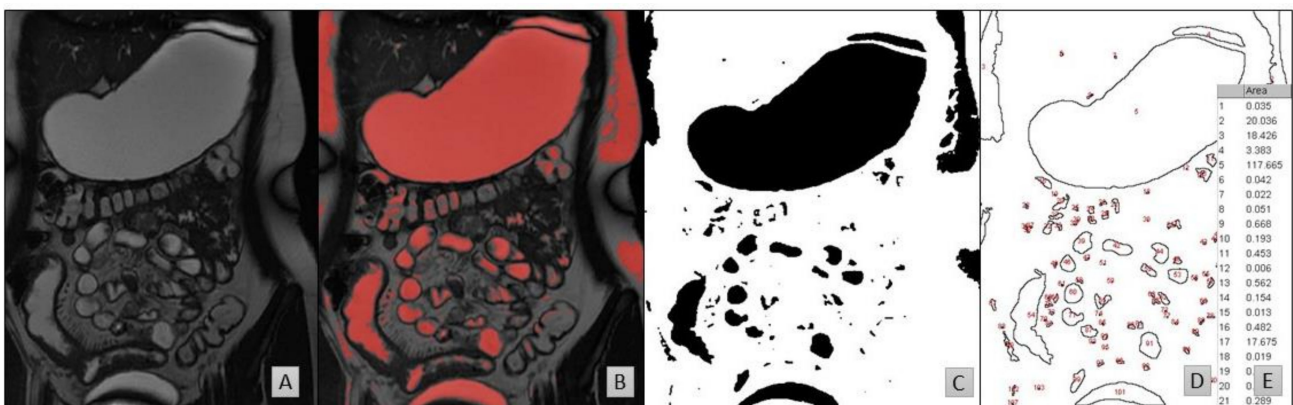


Figure 1. MRI slices taken from a 16-year-old fed female. (A) The original MRI slice. (B) The same slice after thresholding in Horos based on the CSF. (C) The same slice after filtering the red pixels on a black-on-white print in ImageJ. (D) The results of particle analysis show the outlines of the regions of interest and (E) an example extract of the data generated following calculation of the respective areas from (D).

2.2.2. Three-Dimensional Protocol

Two software packages were used to calculate the number of fluid pockets in addition to quantifying the free fluid volume via a 3D-model (Figure 2):

1. Horos to identify and highlight the fluid pockets in the MRI dataset;
2. Blender to remove artefacts and isolate and compute the fluid pockets.

In order to measure individual fluid pockets within the colon, the MRI dataset after the CSF-based thresholding was converted into a 3D-model. Initially, the 3D-volume rendering feature within Horos was used (Figure 2A), which takes the slice thickness and interstitial slice gaps into account. Subsequently, within the colon, the highlighted free fluid areas were approximately excised using the scissor tool, resulting in a 3D-model showing only the fluid pockets (Figure 2B). This model was then exported as a stereolithography (STL) file (Figure 2C). The software programme Blender was used to manipulate the STL file. Blender is a free and open-source 3D-creation suite, released under the GNU General Public License. Blender was used to refine the excision of the colon and remove any non-colon remaining artefacts within the 3D-model, as well as to calculate the volume of each individual pocket. After fixing the scale within Blender to the scale of the MRI image, the fluid pockets volumes were measured by using the plug-in “Mesh—3D print toolbox” in

Blender (Figure 2D). The volume was measured for each individual fluid pocket via the volume feature. The sum of all individual fluid pockets gave the number of pockets for the entire dataset, as well as a second (alternative) measurement of the fluid volume within the paediatric dataset.

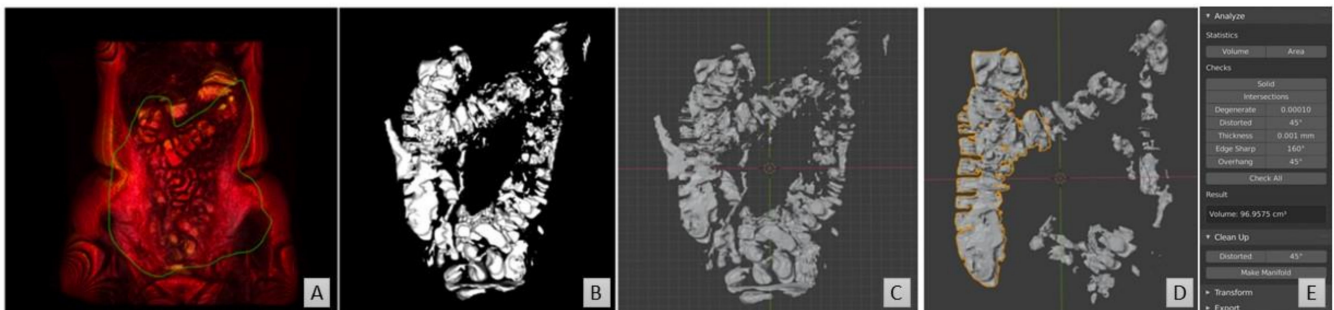


Figure 2. Representative images from the 3D protocol, MRI dataset taken from a 15-year-old female. (A) The 3D rendering in Horos builds a 3D model of the entire dataset. (B) The colon was excised from the 3D model in Horos. (C) The model converted into an STL file and opened in Blender. (D) Non-colon artefacts are removed. (E) The volume of the individual pockets is calculated in Blender.

2.3. Statistical Analysis

SPSS [50] was used for statistical analysis. A statistical test was deemed significant if the p -value (p) was smaller than 0.05. To investigate correlations, Pearson's correlation tests were used. To compare between two groups (such as investigating feed state), independent sample t -tests were used. Where multiple groups were compared, a one-way ANOVA with Bonferroni correction was used. Where multiple measurements on the same participants were investigated (such as a difference in volume in the three colon segments), an ANOVA of repeated measures with a Greenhouse–Geisser correction and post hoc Bonferroni correction was used.

3. Results

3.1. Participant Demographics

The participants MRI datasets were stratified into age groups according to the International Council for Harmonisation of Technical Requirements for Pharmaceuticals for Human Use (ICH) classifications [51,52] (Table 3) with the cohort younger than 2 years old named as infants collectively. Detailed metadata (specific age, weight and sex) for six participants were missing, although their ICH age group was known. Subsequently, these datapoints were excluded from analyses that included sex or specific age. Furthermore, four more datasets were excluded from the 3D-based determination of fluid volume and number of pockets, as they were incompatible with the Blender protocol. Data on threshold values, fluid volumes via both protocols and number of pockets in the total and segments of the colon per participant is available in Table S2.

Table 3. Demographics of the participants included in this study [4].

Age Range	Number of Datasets Available	
	Fasted Children	Fluid-Fed Children
<2 years (neonate/infant/toddler)	9	0
2–5 years (pre-school children)	12	0
6–11 years (school-age children)	6	2
12–16 years (adolescents)	1	16

3.2. Colonic Fluid Volume and Number of Pockets

The paediatric colon contained an average of 22.5 (± 41.3 standard deviation) mL of fluid in 15.5 (± 17.5 standard deviation) discreet fluid pockets; the data were not normally distributed, and the median volume was 0.80 mL with a median number of 12 pockets (Table 4).

Table 4. Fluid volumes and number of pockets for the total, ascending, transverse and descending colon.

Colon Segment	Total	Ascending	Transverse	Descending
Mean \pm SD (mL)	22.48 \pm 41.30	16.44 \pm 27.62	3.78 \pm 11.49	2.27 \pm 7.09
Median (mL)	0.80	0.63	0.004	0.003
Interquartile range (mL)	19.69	18.52	0.65	0.12
Range (min-max) (mL)	0–167.47	0–102.30	0–56.87	0–37.94
Mean \pm SD number of fluid pockets	15.5 \pm 17.5	14.5 \pm 16.4	1.0 \pm 2.5	0.05 \pm 0.2
Median number of fluid pockets	12	10	0	0

The majority of the fluid pockets were small (i.e., volume smaller than 1 mL); a total of 90.4% of the pockets (557/616) were smaller than 1 mL, which accounted for 5.5% of the total fluid volume (51.5 mL/933.2 mL) in the database. The other 9.6% of the pockets (59/616) were larger than 1 mL and contributed 94.5% to the total fluid volume (881.7 mL/933.2 mL) in the database. The paediatric colon contained on average 3.6 ± 2.9 pockets larger than 1 mL (Table 5).

Table 5. Mean and median number and volumes of pockets per participant.

	All Pockets		Pockets Bigger than 1 mL	
	Number per Participant	Volume (mL)	Number per Participant	Volume (mL)
Mean \pm SD	15.5 \pm 17.5	1.52 \pm 12.09	3.6 \pm 2.9	14.60 \pm 36.29
Median	12	0.04	3	3.31

There was a large variation observed in the datasets, both in fluid volume and number and size of pockets. No colonic fluid was found in nine participants, whereas eight datapoints with a total fluid volume higher than 60 mL were classified as statistical outliers, however these were not excluded from the subsequent analysis (shown as open symbols in Figure 3A). The nine participants with no visible fluid had no common demographic factor (age group, sex, fed state), neither did the eight participants with a colon fluid volume higher than 60 mL.

There was a trend for decreased fluid volume in the segments towards the distal colon (Figure 3B). The fluid volumes of the colonic ascending, transverse and descending segments were positively correlated to each other (Pearson's coefficient > 0.58 , $p < 0.001$ in all cases). ANOVA of repeated measures with a Greenhouse–Geisser correction and post hoc Bonferroni correction showed that the ascending colon contained the most fluid ($p < 0.001$). No statistically significant difference was detected between the fluid volumes in the two other segments. However, in four MRI datasets (with the total volume ranging from 0.004 mL to 0.4 mL) either the transverse or descending colon contained all the fluid (and thus none was present in the ascending colon).

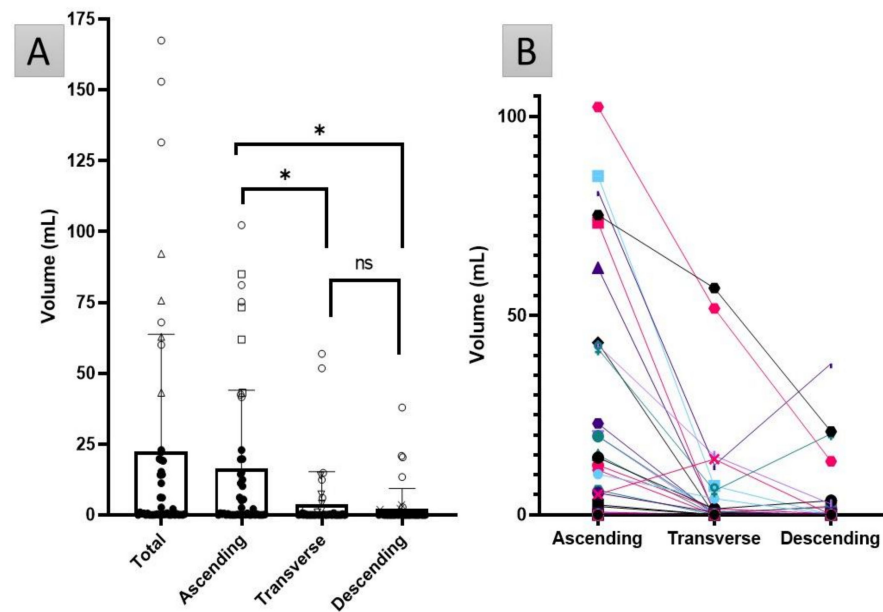


Figure 3. (A) The fluid volume in the total colon and the ascending, transverse and descending segments. The open symbols indicate the individual datapoints that are statistical outliers: circles are outliers in every section, the other symbols indicate outliers only in that particular segment (triangles in the total colon: squares for the ascending colon, triangles for the transverse colon and crosses for the descending colon). The bar chart shows mean values, with standard deviation as the error bar. The * represents a significant difference ($p < 0.05$); ns = not significant. (B) Colon fluid volume in each segment of the colon, linked per participant.

The ascending colon contained the most fluid pockets compared with the other two segments ($p < 0.001$); no statistically significant difference was found in the number of fluid pockets between the transverse and descending colon. Only the ascending colon contained fluid pockets larger than 1 mL, apart from one dataset where a pocket of 249.6 mL was observed that spanned the entire colon. A graphical representation of the distribution of the individual pockets in the entire colon with a volume of up to 25 mL is shown in Figure 4.

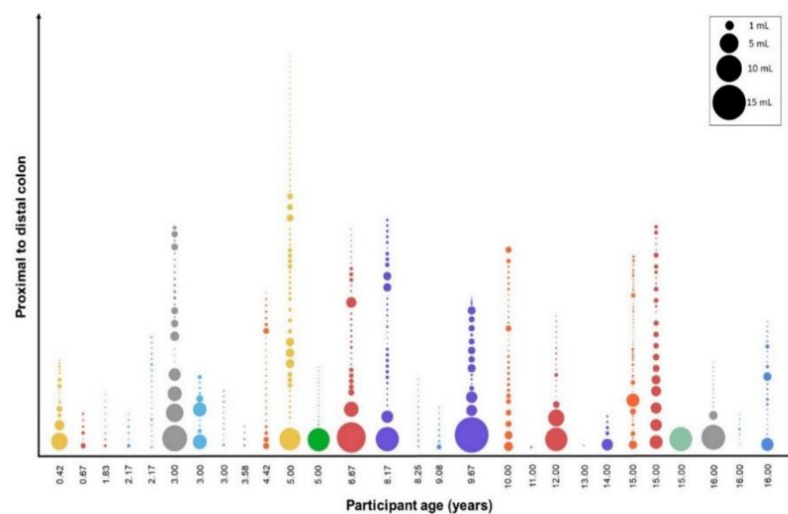


Figure 4. Representation of fluid pockets in the paediatric colon for each participant arranged in order of increasing age. Each bubble depicts an individual fluid pocket, the size illustrates the relative volume. The nine pockets larger than 25 mL, found in nine individual datasets, are not shown, as they distort the scale.

No correlation was detected in the entire cohort between age and the fluid volumes or number of pockets in the total colon or segments ($p > 0.17$ in all cases, Figure 5A). However, in the preschool population (2–5 years old, $n = 11$), age was positively correlated (Pearson's coefficient > 0.65) to total and ascending colonic fluid volume (for both $p < 0.03$, Figure 5B), but no correlation was found between age and the number of fluid pockets.

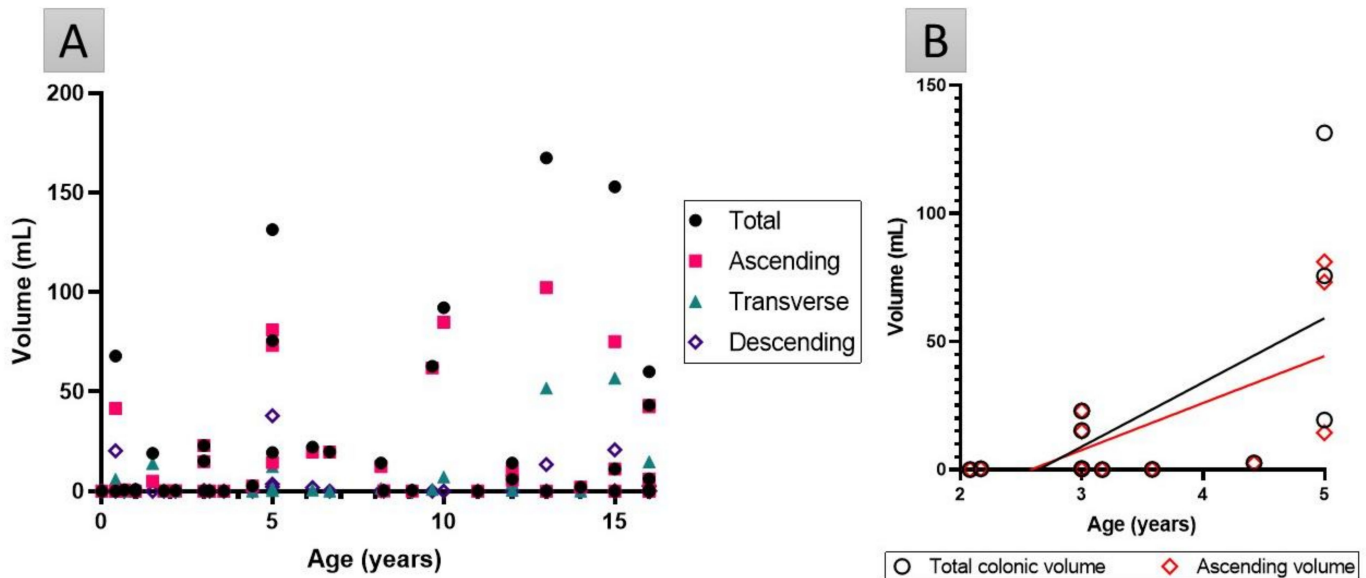


Figure 5. (A) Fluid volume in the total and segments of the colon for every participant as a function of age. No correlations were found, ($p > 0.17$ in all cases). (B) Fluid volume in the total and ascending colon in the preschool population are significantly correlated to age (Pearson's coefficient > 0.65 , $p < 0.03$).

No significant differences in fluid volumes or the number of pockets were detected based on fed state, sex or age group.

3.3. Robustness of Protocol

There was good similarity in threshold values and total fluid volumes between the two operators (Pearson's correlation > 0.97 and $p < 0.001$ in both comparisons, Figure S2), demonstrating the absence of operator-bias. Furthermore, the fluid volumes obtained via the ImageJ protocol were in good correlation to the 3D-based protocol (Pearson's correlation 0.94 , $p < 0.001$, Figure S1). There were no correlations between threshold value and any of the fluid volumes or the number of pockets, demonstrating robustness of the followed protocol (Table S3).

4. Discussion

This study is the first to report fluid volumes in the paediatric colon using MRI quantification. The median fluid volume found in the total colon was 0.80 mL, the mean 22.48 mL \pm 41.30 mL, with a range of 0 mL to 167.5 mL (Table 4). A comparison of these data to other paediatric colonic volumes could also not be made due to a lack of available data [36].

The median paediatric colonic fluid value (0.80 mL) is considerably lower than that observed in adults (2 mL [32] or 8 mL [31]), indicating the colonic fluid volumes are different in children. However, the mean results from this paediatric study are comparable to values reported for the adult colon (Figure 6), which was surprising as the physiology of the colon changes with age.

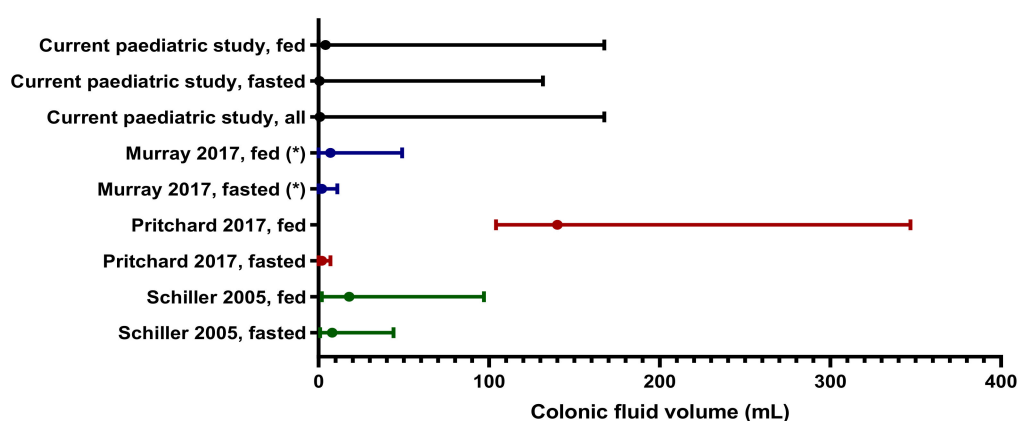


Figure 6. Comparison of the median (closed dot) with associated range reported for colon volumes in adult studies with healthy volunteers. (*): Note that for Murray et al., 2017, the mean instead of median is reported.

The median total colonic volume (TCV) of healthy children aged 14–18 years is reported to be 227 mL (interquartile range 180 mL–263 mL) [53], whereas the mean healthy adult TCV is 760 mL (with a 95% confidence interval of 662 mL–858 mL) [27,54]. Similarly, the length of the colon increases with age, from 52 cm length in children younger than 2 years of age to 150 cm in adults [55]. Therefore, a smaller colonic free fluid volume in the paediatric colon compared with an adult cohort is expected. However, not all colonic parameters change with maturation, e.g., the pH of the paediatric colon children aged 8–14 years is reported to be comparable to adult values [56,57]. Similarly, no significant difference was detected in the fluid volumes between the four different paediatric age groups, (consistent with the existing data on small intestinal fluid volumes) in children [4].

As the generic ICH-classification is based on days/months/years after birth, stratification on a parameter that considers the physicochemical properties of GIT anatomy and contents might have been more appropriate, such as height, body surface area (BSA) or body mass index (BMI) as these are typically used for dose adjustments. However, such data were not collected from the participants. A limitation in this study is that data were only available from 49 patients, extracted from two tertiary centres with differing MRI acquisition protocols. Paediatric MRI small bowel is a scarce resource offered mainly in tertiary centres (UHCW and BCH). It is a specialist modality only performed on selected cases, following discussion at a small bowel multidisciplinary meeting and requires interpretation by specialists. Therefore, the number of paediatric small bowel available for scientific study is small when compared with their adult counterparts. Together, these factors led to a small sample size and even smaller sub-sample size, when comparisons were made based on fed-status, sex or age; in addition to this, the numbers of participants in these sub-groups were not well balanced that may introduce bias into the statistical analysis and interpretation from these groups. Although the sample size is statistically small, it is sizeable considering population type and complexity of the modality; as such, these data should be viewed as preliminary where a larger, well defined cohort is warranted to provide robust data that will lead to more conclusive claims.

As the influence of age was investigated by comparing four paediatric age groups, the sample size per age group was similar to sample sizes used in the previous studies on healthy adult volunteers. However, the demographics of the participants in the adult studies were closely controlled; for example, those in Murray et al. [3] ($n = 12$) were all 20–22 years old and healthy, to minimise variability in the dataset. The paediatric participants have potential underlying morbidities, resulting in variability which may have introduced bias into the data. The large variability in colon fluid volumes was also observed in studies on healthy adults via MRI quantification [32,42,58,59]. The variability in studies undertaken using a small group of healthy volunteers in a clinical setting are less likely to capture the real-world variability, compared with studies in a heterogenous paediatric population with potential comorbidities [38,60].

There were on average 3.6 ± 2.9 fluid pockets larger than 1 mL, mainly in the ascending colon. Similarly to adults, the majority of the fluid pockets were very small [3] (Figures 4 and 7). In this study, it was found that only 9.6% of the fluid pockets were larger than 1 mL, yet they contributed for 94.5% to the overall volume quantified. The software protocols used in this study did not use any limits on the size of fluid pockets to be quantified, therefore even fluid pockets of 0.01 mL were included in the data. As 90.4% of the fluid pockets were smaller than 1 mL and contributed to only 5.5% of the fluid observed in the study (55.5 mL), their physiological relevance in colonic absorption might be questioned.

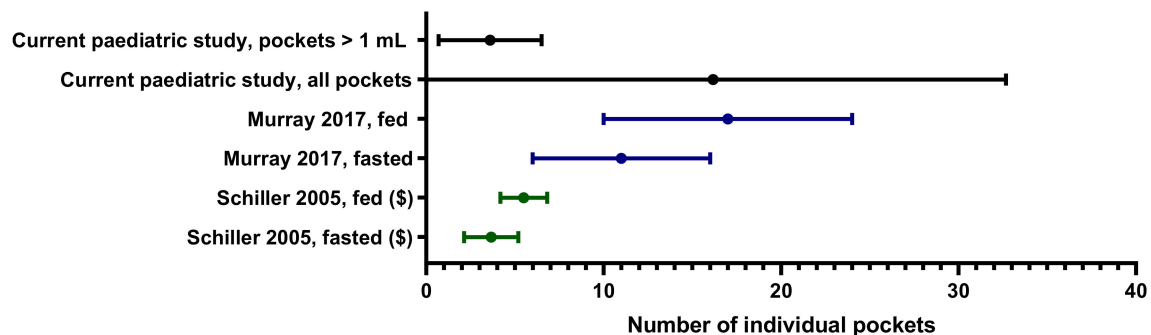


Figure 7. Comparison of the mean and SD reported for the number of fluid pockets in the colon in adult studies with healthy volunteers. (\$): Note that for Schiller et al., 2005, the 25% and 75% percentiles are reported instead of the SD.

No correlation was observed between colonic fluid volumes or the number of pockets, and age or weight. This implies that age or weight does not correlate to colonic fluid volumes, which is in contrast with other GIT parameters such as gastric pH [1] or the need for fluid intake [51] where the most significant changes are observed in neonates and infants (<2 years) [61]. Current dosage guidelines use allometric scaling based on age, weight or BSA to extrapolate paediatric doses from adult data [37,51,62–65]. Further investigation is required to investigate the appropriateness of allometric scaling for colon-specific drug delivery systems colon (CDDS) [37], especially for poorly soluble drugs that act within the colon. Only in the preschool category (children aged 2–5 years, $n = 12$), was age significantly positively correlated to fluid in the total and the ascending colon (Figure 5B). This implies that children in this category will have more fluid in their ascending (and thus total) colon as they are closer to 5 years of age; this finding could be due to the small sample size and the large variability seen within these 12 participants.

Fed status had no impact on fluid volumes (data not shown), which could be a result of several factors. Firstly, it was unlikely that Oral Klean Prep had an impact on the colon fluid volumes in the timeframe of this study, although an effect could not be excluded a priori, as literature is conflicting about when an ingested solution reaches the colon since this is subjected to inter- and intra-variability [27]. In addition, Oral Klean Prep is an osmotic laxative, which draws water into the GIT. Therefore, it is not fully representative to a fluid-fed child. Placidi et al. [66] reported a significant increase in ascending colon fluid volumes 45 min post-ingestion [66] of 5% mannitol (another osmotic laxative) in 350 mL of water, so a possible effect could not be excluded in advance. The healthy paediatric population is believed to have a gastric emptying rate [67] and small intestinal transit time (SITT) comparable to adults (SITT $3.49 \text{ h} \pm 1.02 \text{ h}$ (mean \pm SD)) based on meta-analysis [38,65,68], although data suggest children younger than 2 years of age have a slower (longer) SITT [38,51]. In addition, this meta-SITT was not affected by fed state [68]. The meta-gastric emptying rate and meta-SITT values support the absence of an impact of Oral Klean Prep on the colon volumes as observed in this study. The increase of the free fluid in the colon of fasted adults Pritchard et al. [32] observed 60 min post-ingestion of 500 mL Moviprep or Murray et al. [3] noticed 30 min post-ingestion of a 240 mL glass water is likely to be due to the gastrocolonic reflex, as hypothesised by Lemmens et al. [69].

Secondly, there was no verification of fed state prior to analysis as this study had a real-world setting. The consumption of the full 500 mL Oral Klean Prep was not monitored. In addition, it was not strictly monitored whether the children in the fasted population indeed fasted overnight, although this was part of their clinical instructions. Tighter monitoring on the clinical protocols prior to MRI with specific reference to fasting and ingestion of the solution would improve the interpretation of this MRI data.

The ascending colon typically contained the highest portion of fluid (Figure 3). Correlations demonstrated that when fluid is present in the ascending colon, this can act as a predictor for the total colonic volume. The same trend was observed in adults [3,27]. Consequently, as chyme from the small intestine enters the colon, the desiccating function of the colon to transform chyme to drier stools explains this trend [36], where less water is identified in more distal regions. It should be noted that only the free-flowing water is being quantified, based on the fluidity of the CSF [42].

There is substantial variation in the choice of software used to interrogate MRI datasets in order to calculate fluid volumes and pockets [3,4,31,32,42,45,58]. Previous studies have already expressed the need for standardisation of methods [26], as the CSF-based threshold for free fluid is dataset dependent. However, no influence of CSF-threshold values to the obtained data in this study was detected, consistent with literature [3,4,31,42]. In addition, cross-analysis of the extracted values between the 2D- and 3D-based protocol and between multiple operators shows that both protocols produce similar results regardless of operator or used modelling approach (Figures S1–S3). Therefore, the use of CSF-based thresholds on the MRI datasets are robust and provide consistent results for colonic fluid analysis.

This pioneering study quantified the free fluid in the paediatric colon, which is of great interest to the pharmaceutical industry [27] for paediatric drug development as clinical studies in the paediatric population often face ethical restrictions [30,36]. Although most data currently available for *in silico* models are derived from healthy Caucasian adults, accurate physiological data derived from the intended patient population are more appropriate for biorelevant modelling [35,70], e.g., to account for an altered GIT physiology due to disease or age [38]. For the first time, *in vitro* and *in silico* models can be developed tailored to the paediatric cohort [36,38] that are informed by real-world data on the volume of fluid (mean, median, extreme values and variability) within the paediatric colon.

5. Conclusions

This study successfully quantified the fluid volumes within the paediatric colon. Two methods were employed to quantify fluid in MRI datasets and their robustness was demonstrated via cross-analysis between operators and methods.

The small overall sample size and even smaller sub-population sizes meant that these data are preliminary, and a fuller cohort study is required to verify the findings presented here. The median fluid volume for the total paediatric colon (0.80 mL) is comparable to literature data for the adult colon, although the mean paediatric volume (22.48 ± 41.30 mL) is nearly double than the adult value standardly used, i.e., 13 mL. The high variability was also observed in adults. No overall correlation was detected between colonic fluid volumes and age, similar to results in the paediatric SI. Fed status, sex or age across the whole population did not influence the colon fluid volumes. The fact that a significant correlation was observed in the 2–5 years group (who were all fasted) between age and fluid volumes in the entire and ascending colon warrants further investigation. No such correlation was observed for other age groups. Furthermore, the ascending colon contained the most fluid compared with the transverse and descending colon. This study demonstrates the feasibility of obtaining real-world data from MRI to inform physiologically based models, which minimises the burden to special populations.

The novel output from this study will improve the physiological understanding of the paediatric colon, aid biopredictive *in silico* simulations and establishing novel, more accurate *in vitro* assays and thus support paediatric drug development that targets the colon, resulting in more age-appropriate medicines for the paediatric population [71,72].

Supplementary Materials: The following are available online at <https://www.mdpi.com/article/10.3390/pharmaceutics13101729/s1>, Table S1: Data on participants demographics and MRI set-up. Table S2: Data on used threshold values, fluid volumes via both protocols and number of pockets in the total and segments of the colon per participant, Table S3: correlation of threshold with volumes and number of pockets. Figure S1: correlation of the fluid volumes in the total colon on the same datasets between the 2D- and 3D-protocol. Figure S2: correlation of fluid volume in the total colon on the same datasets via the 2D-protocol between operators A and B. Figure S3: correlation between the CSF-threshold set on the same datasets between operators A and B.

Author Contributions: J.G., G.P., R.D.H. and H.K.B. designed the study. J.G. and B.A. analysed the image data, with assistance of H.E.W. and E.E. The manuscript was written by J.G., B.A., R.D.H. and H.K.B. All authors have read and agreed to the published version of the manuscript.

Funding: This research was funded by Certara UK Limited, Simcyp Academic Awards, Grant and Partnership Scheme (GPS).

Institutional Review Board Statement: The study was conducted in accordance with the Declaration of Helsinki, and the protocol was ethically approved: REC reference: 18/EM/0251 (IRAS 237159 MRI: Fluid volumes and localisation in paediatric GI tract, approval date 22 August 2018).

Informed Consent Statement: All subjects gave their informed consent for inclusion before they participated in the study.

Acknowledgments: Birmingham Children's Hospital (BCH) and University Hospitals Coventry and Warwickshire NHS Trust (UHCW) are thanked for providing the paediatric datasets. Papadatou-Soulou is thanked for her contribution for providing the datasets and assisting in set-up of the analysis. Charlotte Goelen is thanked for her contribution in providing access to Horos.

Conflicts of Interest: The authors declare no conflict of interest.

Abbreviations

MRI, magnetic resonance imaging; GIT, gastrointestinal tract; XR, extended release; PBPK, physiologically based pharmacokinetic; BCH, Birmingham Children's Hospital; UHCW, University Hospitals Coventry and Warwickshire; CSF, cerebrospinal fluid; ICH, International Council for Harmonisation of Technical Requirements for Pharmaceuticals for Human Use; STL, stereolithography; BSA, body surface area; BMI, body mass index; SITT, small intestinal transit time; UBL, unstirred boundary layer.

References

1. Batchelor, H.K.; Fotaki, N.; Klein, S. Paediatric oral biopharmaceutics: Key considerations and current challenges. *Adv. Drug Deliv. Rev.* **2014**, *73*, 102–126. [[CrossRef](#)] [[PubMed](#)]
2. Batchelor, H.K.; Marriott, J.F. Paediatric pharmacokinetics: Key considerations. *Br. J. Clin. Pharmacol.* **2015**, *79*, 395–404. [[CrossRef](#)]
3. Murray, K.; Hoad, C.L.; Mudie, D.M.; Wright, J.; Heissam, K.; Abreghart, N.; Pritchard, S.E.; Al Atwah, S.; Gowland, P.A.; Garnett, M.C.; et al. Magnetic Resonance Imaging Quantification of Fasted State Colonic Liquid Pockets in Healthy Humans. *Mol. Pharm.* **2017**, *14*, 2629–2638. [[CrossRef](#)] [[PubMed](#)]
4. Papadatou-Soulou, E.; Mason, J.; Parsons, C.; Oates, A.; Thyagarajan, M.; Batchelor, H.K. Magnetic Resonance Imaging Quantification of Gastrointestinal Liquid Volumes and Distribution in the Gastrointestinal Tract of Children. *Mol. Pharm.* **2019**, *16*, 3896–3903. [[CrossRef](#)] [[PubMed](#)]
5. Vertzoni, M.; Augustijns, P.; Grimm, M.; Koziolok, M.; Lemmens, G.; Parrott, N.J.; Pentafragka, C.; Reppas, C.; Rubbens, J.; Abeele, J.V.D.; et al. Impact of regional differences along the gastrointestinal tract of healthy adults on oral drug absorption: An UNGAP review. *Eur. J. Pharm. Sci.* **2019**, *134*, 153–175. [[CrossRef](#)] [[PubMed](#)]
6. Mudie, D.M.; Amidon, G.L.; Amidon, G.E. Physiological parameters for oral delivery and in vitro testing. *Mol. Pharm.* **2010**, *7*, 1388–1405. [[CrossRef](#)]
7. Stamatopoulos, K.; Karandikar, S.; Goldstein, M.; O'Farrell, C.; Marciari, L.; Sulaiman, S.; Hoad, C.L.; Simmons, M.J.H.; Batchelor, H.K. Dynamic Colon Model (DCM): A Cine-MRI Informed Biorelevant In Vitro Model of the Human Proximal Large Intestine Characterized by Positron Imaging Techniques. *Pharmaceutics* **2020**, *12*, 659. [[CrossRef](#)] [[PubMed](#)]
8. Amidon, S.; Brown, J.E.; Dave, V.S. Colon-Targeted Oral Drug Delivery Systems: Design Trends and Approaches. *AAPS PharmSciTech* **2015**, *16*, 731–741. [[CrossRef](#)]
9. Karalis, V.; Magklara, E.; Shah, V.P.; Macheras, P. From Drug Delivery Systems to Drug Release, Dissolution, IVIVC, BCS, BDDCS, Bioequivalence and Biowaivers. *Pharm. Res.* **2010**, *27*, 2018–2029. [[CrossRef](#)] [[PubMed](#)]

10. De Corte, T.; Janssens, E.; D'Hondt, A.; Thorrez, K.; Arts, J.; Dejaegher, K.; D'Heygere, F.; Holvoet, A.; Van Besien, B.; Harlet, L.; et al. Beclomethasone dipropionate in microscopic colitis: Results of an exploratory open-label multicentre study (COLCO). *United Eur. Gastroenterol. J.* **2019**, *7*, 1183–1188. [[CrossRef](#)]
11. Philip, A.; Philip, B. Colon Targeted Drug Delivery Systems: A Review on Primary and Novel Approaches. *Oman Med. J.* **2010**, *25*, 70–78. [[CrossRef](#)] [[PubMed](#)]
12. Zhang, M.; Merlin, D. Nanoparticle-Based Oral Drug Delivery Systems Targeting the Colon for Treatment of Ulcerative Colitis. *Inflamm. Bowel Dis.* **2018**, *24*, 1401–1415. [[CrossRef](#)] [[PubMed](#)]
13. Verrotti, A.; Salladini, C.; Di Marco, G.; Piscicella, F.; Chiarelli, F. Extended-Release Formulations in Epilepsy. *J. Child Neurol.* **2007**, *22*, 419–426. [[CrossRef](#)] [[PubMed](#)]
14. Garbacz, G.; Klein, S. Dissolution testing of oral modified-release dosage forms. *J. Pharm. Pharmacol.* **2012**, *64*, 944–968. [[CrossRef](#)] [[PubMed](#)]
15. Dubey, S.K.; Parab, S.; Dabholkar, N.; Agrawal, M.; Singhvi, G.; Alexander, A.; Bapat, R.A.; Kesharwani, P. Oral peptide delivery: Challenges and the way ahead. *Drug Discov. Today* **2021**, *26*, 931–950. [[CrossRef](#)] [[PubMed](#)]
16. Del Curto, M.D.; Maroni, A.; Foppoli, A.; Zema, L.; Gazzaniga, A.; Sangalli, M.E. Preparation and evaluation of an oral delivery system for time-dependent colon release of insulin and selected protease inhibitor and absorption enhancer compounds. *J. Pharm. Sci.* **2009**, *98*, 4661–4669. [[CrossRef](#)]
17. Chey, W.D.; Sayuk, G.S.; Bartolini, W.; Reasner, D.S.; Fox, S.M.; Bochenek, W.; Boinpally, R.; Shea, E.; Tripp, K.; Borgstein, N. Randomized Trial of 2 Delayed-Release Formulations of Linaclotide in Patients With Irritable Bowel Syndrome With Constipation. *Am. J. Gastroenterol.* **2021**, *116*, 354–361. [[CrossRef](#)]
18. Wilson, C.G. The transit of dosage forms through the colon. *Int. J. Pharm.* **2010**, *395*, 17–25. [[CrossRef](#)]
19. Ye, B.; van Langenberg, D.R. Mesalazine preparations for the treatment of ulcerative colitis: Are all created equal? *World J. Gastrointest. Pharmacol. Ther.* **2015**, *6*, 137–144. [[CrossRef](#)]
20. Fotaki, N.; Vertzoni, M. Biorelevant dissolution methods and their applications in in vitro in vivo correlations for oral formulations. *Open Drug Deliv. J.* **2010**, *4*, 2–13. [[CrossRef](#)]
21. Löbenberg, R.; Krämer, J.; Shah, V.P.; Amidon, G.L.; Dressman, J.B. Dissolution testing as a prognostic tool for oral drug absorption: Dissolution behavior of glibenclamide. *Pharm. Res.* **2000**, *17*, 439–444. [[CrossRef](#)] [[PubMed](#)]
22. Jantratid, E.; De Maio, V.; Ronda, E.; Mattavelli, V.; Vertzoni, M.; Dressman, J.B. Application of biorelevant dissolution tests to the prediction of in vivo performance of diclofenac sodium from an oral modified-release pellet dosage form. *Eur. J. Pharm. Sci.* **2009**, *37*, 434–441. [[CrossRef](#)]
23. Lemmens, G.; Brouwers, J.; Snoeys, J.; Augustijns, P.; Vanuytsel, T. Insight into the colonic disposition of celecoxib in humans. *Eur. J. Pharm. Sci.* **2020**, *145*, 105242. [[CrossRef](#)] [[PubMed](#)]
24. Lemmens, G.; Brouwers, J.; Snoeys, J.; Augustijns, P.; Vanuytsel, T. Insight into the Colonic Disposition of Sulindac in Humans. *J. Pharm. Sci.* **2021**, *110*, 259–267. [[CrossRef](#)] [[PubMed](#)]
25. Fotaki, N.; Aivaliotis, A.; Butler, J.; Dressman, J.; Fischbach, M.; Hempenstall, J.; Klein, S.; Reppas, C. A comparative study of different release apparatus in generating in vitro–in vivo correlations for extended release formulations. *Eur. J. Pharm. Biopharm.* **2009**, *73*, 115–120. [[CrossRef](#)]
26. Pasta, S.; Gentile, G.; Raffa, G.M.; Scardulla, F.; Bellavia, D.; Luca, A.; Pilato, M.; Scardulla, C. Three-dimensional parametric modeling of bicuspid aortopathy and comparison with computational flow predictions. *Artif. Organs* **2017**, *41*, E92–E102. [[CrossRef](#)]
27. Sulaiman, S.; Marciani, L. MRI of the Colon in the Pharmaceutical Field: The Future before us. *Pharmaceutics* **2019**, *11*, 146. [[CrossRef](#)] [[PubMed](#)]
28. Georgaka, D.; Butler, J.; Kesisoglou, F.; Reppas, C.; Vertzoni, M. Evaluation of Dissolution in the Lower Intestine and Its Impact on the Absorption Process of High Dose Low Solubility Drugs. *Mol. Pharm.* **2017**, *14*, 4181–4191. [[CrossRef](#)]
29. Vertzoni, M.; Diakidou, A.; Chatziliadis, M.; Söderlind, E.; Abrahamsson, B.; Dressman, J.B.; Reppas, C. Biorelevant Media to Simulate Fluids in the Ascending Colon of Humans and Their Usefulness in Predicting Intracolonic Drug Solubility. *Pharm. Res.* **2010**, *27*, 2187–2196. [[CrossRef](#)] [[PubMed](#)]
30. Johnson, T.N.; Zhou, D.; Bui, K.H. Development of physiologically based pharmacokinetic model to evaluate the relative systemic exposure to quetiapine after administration of IR and XR formulations to adults, children and adolescents. *Biopharm. Drug Dispos.* **2014**, *35*, 341–352. [[CrossRef](#)] [[PubMed](#)]
31. Schiller, C.; Frohlich, C.-P.; Giessmann, T.; Siegmund, W.; Monnikes, H.; Hosten, N.; Weitschies, W. Intestinal fluid volumes and transit of dosage forms as assessed by magnetic resonance imaging. *Aliment. Pharmacol. Ther.* **2005**, *22*, 971–979. [[CrossRef](#)]
32. Pritchard, S.E.; Paul, J.; Major, G.; Marciani, L.; Gowland, P.A.; Spiller, R.C.; Hoad, C.L. Assessment of motion of colonic contents in the human colon using MRI tagging. *Neurogastroenterol. Motil.* **2017**, *29*, e13091. [[CrossRef](#)] [[PubMed](#)]
33. Tsume, Y.; Patel, S.; Fotaki, N.; Bergström, C.; Amidon, G.L.; Brasseur, J.G.; Mudie, D.M.; Sun, D.; Bermejo, M.; Gao, P.; et al. In Vivo Predictive Dissolution and Simulation Workshop Report: Facilitating the Development of Oral Drug Formulation and the Prediction of Oral Bioperformance. *AAPS J.* **2018**, *20*, 100. [[CrossRef](#)] [[PubMed](#)]
34. Yu, A.; Baker, J.R.; Fioritto, A.F.; Wang, Y.; Luo, R.; Li, S.; Wen, B.; Bly, M.; Tsume, Y.; Koenigsnecht, M.J.; et al. Measurement of in vivo Gastrointestinal Release and Dissolution of Three Locally Acting Mesalamine Formulations in Regions of the Human Gastrointestinal Tract. *Mol. Pharm.* **2017**, *14*, 345–358. [[CrossRef](#)] [[PubMed](#)]

35. Maharaj, A.R.; Edginton, A.N. Physiologically based pharmacokinetic modeling and simulation in pediatric drug development. *CPT Pharmacomet. Syst. Pharmacol.* **2014**, *3*, e150. [CrossRef] [PubMed]
36. Vinarov, Z.; Abrahamsson, B.; Artursson, P.; Batchelor, H.; Berben, P.; Bernkop-Schnürch, A.; Butler, J.; Ceulemans, J.; Davies, N.; Dupont, D.; et al. Current challenges and future perspectives in oral absorption research: An opinion of the UNGAP network. *Adv. Drug Deliv. Rev.* **2021**, *171*, 289–331. [CrossRef] [PubMed]
37. Stillhart, C.; Vučićević, K.; Augustijns, P.; Basit, A.W.; Batchelor, H.; Flanagan, T.R.; Gesquiere, I.; Greupink, R.; Keszthelyi, D.; Koskinen, M.; et al. Impact of gastrointestinal physiology on drug absorption in special populations—An UNGAP review. *Eur. J. Pharm. Sci.* **2020**, *147*, 105280. [CrossRef]
38. Vinarov, Z.; Abdallah, M.; Agundez, J.; Allegaert, K.; Basit, A.W.; Braeckmans, M.; Ceulemans, J.; Corsetti, M.; Griffin, B.; Grimm, M.; et al. Impact of gastrointestinal tract variability on oral drug absorption and pharmacokinetics: An UNGAP review. *Eur. J. Pharm. Sci.* **2021**, *162*, 105812. [CrossRef] [PubMed]
39. Zhang, X.; Duan, J.; Kesisoglou, F.; Novakovic, J.; Amidon, G.; Jamei, M.; Lukacova, V.; Eissing, T.; Tsakalozou, E.; Zhao, L.; et al. Mechanistic Oral Absorption Modeling and Simulation for Formulation Development and Bioequivalence Evaluation: Report of an FDA Public Workshop. *CPT Pharmacomet. Syst. Pharmacol.* **2017**, *6*, 492–495. [CrossRef]
40. Nicolas, J.-M.; Bouzom, F.; Hugues, C.; Ungell, A.-L. Oral drug absorption in pediatrics: The intestinal wall, its developmental changes and current tools for predictions. *Biopharm. Drug Dispos.* **2017**, *38*, 209–230. [CrossRef] [PubMed]
41. Yu, G.; Zheng, Q.-S.; Li, G.-F. Similarities and Differences in Gastrointestinal Physiology Between Neonates and Adults: A Physiologically Based Pharmacokinetic Modeling Perspective. *AAPS J.* **2014**, *16*, 1162–1166. [CrossRef]
42. Mudie, D.M.; Murray, K.; Hoad, C.L.; Pritchard, S.E.; Garnett, M.C.; Amidon, G.L.; Gowland, P.A.; Spiller, R.C.; Amidon, G.E.; Marciani, L. Quantification of Gastrointestinal Liquid Volumes and Distribution Following a 240 mL Dose of Water in the Fasted State. *Mol. Pharm.* **2014**, *11*, 3039–3047. [CrossRef] [PubMed]
43. Pritchard, S.E.; Marciani, L.; Garsed, K.C.; Hoad, C.; Thongborisute, W.; Roberts, E.; Gowland, P.; Spiller, R.C. Fasting and postprandial volumes of the undisturbed colon: Normal values and changes in diarrhea-predominant irritable bowel syndrome measured using serial MRI. *Neurogastroenterol. Motil.* **2014**, *26*, 124–130. [CrossRef]
44. The Horos Project. Horos is a free and open source code software (FOSS) program that is distributed free of charge under the LGPL license at horosproject.org and sponsored by Nimble Co LLC d/b/a Purview in Annapolis, MD, USA. Available online: <https://horosproject.org/faqs/> (accessed on 5 September 2021).
45. Hoad, C.L.; Marciani, L.; Foley, S.; Totman, J.J.; Wright, J.; Bush, D.; Cox, E.; Campbell, E.; Spiller, R.C.; Gowland, P.A. Non-invasive quantification of small bowel water content by MRI: A validation study. *Phys. Med. Biol.* **2007**, *52*, 6909–6922. [CrossRef]
46. Laqua, R. Global Thresholding v1.0 OsiriX Plugin [Software]. Available online: <https://osirixpluginbasics.wordpress.com/2012/10/30/plugin-global-thresholding/> (accessed on 26 March 2020).
47. Schneider, C.A.; Rasband, W.S.; Eliceiri, K.W. NIH Image to ImageJ: 25 years of image analysis. *Nat. Methods* **2012**, *9*, 671–675. [CrossRef] [PubMed]
48. Grimm, M.; Koziolok, M.; Saleh, M.; Schneider, F.; Garbacz, G.; Kühn, J.-P.; Weitschies, W. Gastric Emptying and Small Bowel Water Content after Administration of Grapefruit Juice Compared to Water and Isocaloric Solutions of Glucose and Fructose: A Four-Way Crossover MRI Pilot Study in Healthy Subjects. *Mol. Pharm.* **2018**, *15*, 548–559. [CrossRef]
49. Sharif, H.; Devadason, D.; Abreheart, N.; Stevenson, R.; Marciani, L. Imaging Measurement of Whole Gut Transit Time in Paediatric and Adult Functional Gastrointestinal Disorders: A Systematic Review and Narrative Synthesis. *Diagnostics* **2019**, *9*, 221. [CrossRef] [PubMed]
50. IBM. Released 2020. In *IBM SPSS Statistics for Windows, Version 27.0*; IBM: Armonk, NY, USA, 2020.
51. Guimarães, M.; Stelova, M.; Holm, R.; Reppas, C.; Symillides, M.; Vertzoni, M.; Fotaki, N. Biopharmaceutical considerations in paediatrics with a view to the evaluation of orally administered drug products—A PEARRL review. *J. Pharm. Pharmacol.* **2019**, *71*, 603–642. [CrossRef]
52. Committee for Medicinal Products for Human Use (CHMP). *Reflection Paper: Formulations of Choice for the Paediatric Population*; EMA: London, UK, 2006; Available online: https://www.ema.europa.eu/en/documents/scientific-guideline/reflection-paper-formulations-choice-paediatric-population_en.pdf (accessed on 5 September 2021).
53. Sharif, H.; Hoad, C.; Abreheart, N.; Gowland, P.; Spiller, R.; Kirkham, S.; Loganathan, S.; Papadopoulos, M.; Benninga, M.; Devadason, D.; et al. Colonic Volume Changes in Paediatric Constipation Compared to Normal Values Measured Using MRI. *Diagnostics* **2021**, *11*, 974. [CrossRef]
54. Nilsson, M.; Sandberg, T.H.; Poulsen, J.L.; Gram, M.; Frøkjær, J.B.; Østergaard, L.R.; Krogh, K.; Brock, C.; Drewes, A. Quantification and variability in colonic volume with a novel magnetic resonance imaging method. *Neurogastroenterol. Motil.* **2015**, *27*, 1755–1763. [CrossRef] [PubMed]
55. Mirjalili, S.A.; Tarr, G.; Stringer, M.D. The length of the large intestine in children determined by computed tomography scan. *Clin. Anat.* **2017**, *30*, 887–893. [CrossRef] [PubMed]
56. Fallingborg, J.; Christensen, L.A.; Ingeman-Nielsen, M.; Jacobsen, B.A.; Abildgaard, K.; Rasmussen, H.H.; Rasmussen, S.N. Measurement of Gastrointestinal pH and Regional Transit Times in Normal Children. *J. Pediatr. Gastroenterol. Nutr.* **1990**, *11*, 211–214. [CrossRef] [PubMed]
57. Broesder, A.; Woerdenbag, H.J.; Prins, G.H.; Nguyen, D.N.; Frijlink, H.W.; Hinrichs, W.L. pH-dependent ileocolonic drug delivery, part I: In vitro and clinical evaluation of novel systems. *Drug Discov. Today* **2020**, *25*, 1362–1373. [CrossRef] [PubMed]

58. Murray, K.A.; Lam, C.; Rehman, S.; Marciani, L.; Costigan, C.; Hoad, C.L.; Lingaya, M.R.; Banwait, R.; Bawden, S.J.; Gowland, P.A.; et al. Corticotropin-releasing factor increases ascending colon volume after a fructose test meal in healthy humans: A randomized controlled trial. *Am. J. Clin. Nutr.* **2016**, *103*, 1318–1326. [[CrossRef](#)] [[PubMed](#)]
59. Wilkinson-Smith, V.; Menys, A.; Bradley, C.; Corsetti, M.; Marciani, L.; Atkinson, D.; Coupland, C.; Taylor, S.A.; Gowland, P.; Spiller, R.; et al. The MRI colonic function test: Reproducibility of the Macrogol stimulus challenge. *Neurogastroenterol. Motil.* **2020**, *32*, e13942. [[CrossRef](#)] [[PubMed](#)]
60. Kim, H.-S.; Lee, S.; Kim, J.H. Real-world Evidence versus Randomized Controlled Trial: Clinical Research Based on Electronic Medical Records. *J. Korean Med. Sci.* **2018**, *33*, e213. [[CrossRef](#)] [[PubMed](#)]
61. Neal-Kluever, A.; Fisher, J.; Grylack, L.; Kakiuchi-Kiyota, S.; Halpern, W. Physiology of the Neonatal Gastrointestinal System Relevant to the Disposition of Orally Administered Medications. *Drug Metab. Dispos.* **2018**, *47*, 296–313. [[CrossRef](#)] [[PubMed](#)]
62. Sanchez, J.M.D.M.; Alvarez, I.G.; Revert, A.C.; Álvarez, M.G.; Ruiz, A.N.; Amidon, G.L.; Bermejo, M.; Sanz, M.B. Biopharmaceutical optimization in neglected diseases for paediatric patients by applying the provisional paediatric biopharmaceutical classification system. *Br. J. Clin. Pharmacol.* **2018**, *84*, 2231–2241. [[CrossRef](#)]
63. DelMoral-Sanchez, J.-M.; Gonzalez-Alvarez, I.; Gonzalez-Alvarez, M.; Navarro, A.; Bermejo, M. Classification of WHO Essential Oral Medicines for Children Applying a Provisional Pediatric Biopharmaceutics Classification System. *Pharmaceutics* **2019**, *11*, 567. [[CrossRef](#)]
64. Gandhi, S.V.; Rodriguez, W.; Khan, M.; Polli, J.E. Considerations for a Pediatric Biopharmaceutics Classification System (BCS): Application to Five Drugs. *AAPS PharmSciTech* **2014**, *15*, 601–611. [[CrossRef](#)]
65. Maharaj, A.R.; Edginton, A.N. Examining Small Intestinal Transit Time as a Function of Age: Is There Evidence to Support Age-Dependent Differences among Children? *Drug Metab. Dispos.* **2016**, *44*, 1080–1089. [[CrossRef](#)] [[PubMed](#)]
66. Placidi, E.; Marciani, L.; Hoad, C.; Napolitano, A.; Garsed, K.C.; Pritchard, S.E.; Cox, E.; Costigan, C.; Spiller, R.; Gowland, P.A. The effects of loperamide, or loperamide plus simethicone, on the distribution of gut water as assessed by MRI in a mannitol model of secretory diarrhoea. *Aliment. Pharmacol. Ther.* **2012**, *36*, 64–73. [[CrossRef](#)] [[PubMed](#)]
67. Bonner, J.J.; Vajjah, P.; Abduljalil, K.; Jamei, M.; Rostami-Hodjegan, A.; Tucker, G.T.; Johnson, T.N. Does age affect gastric emptying time? A model-based meta-analysis of data from premature neonates through to adults. *Biopharm. Drug Dispos.* **2015**, *36*, 245–257. [[CrossRef](#)] [[PubMed](#)]
68. Abuhelwa, A.Y.; Foster, D.; Upton, R. A Quantitative Review and Meta-models of the Variability and Factors Affecting Oral Drug Absorption—Part II: Gastrointestinal Transit Time. *AAPS J.* **2016**, *18*, 1322–1333. [[CrossRef](#)]
69. Lemmens, G.; Van Camp, A.; Kourula, S.; Vanuytsel, T.; Augustijns, P. Drug Disposition in the Lower Gastrointestinal Tract: Targeting and Monitoring. *Pharmaceutics* **2021**, *13*, 161. [[CrossRef](#)]
70. Huang, W.; Lee, S.L.; Yu, L.X. Mechanistic Approaches to Predicting Oral Drug Absorption. *AAPS J.* **2009**, *11*, 217–224. [[CrossRef](#)]
71. Pawar, G.; Wu, F.; Zhao, L.; Fang, L.; Burckart, G.J.; Feng, K.; Mousa, Y.M.; Naumann, F.; Batchelor, H.K. Development of a Pediatric Relative Bioavailability/Bioequivalence Database and Identification of Putative Risk Factors Associated with Evaluation of Pediatric Oral Products. *AAPS J.* **2021**, *23*, 1–12. [[CrossRef](#)] [[PubMed](#)]
72. DelMoral-Sanchez, J.-M.; Gonzalez-Alvarez, I.; Gonzalez-Alvarez, M.; Navarro-Ruiz, A.; Bermejo, M. Availability of Authorizations from EMA and FDA for Age-Appropriate Medicines Contained in the WHO Essential Medicines List for Children 2019. *Pharmaceutics* **2020**, *12*, 316. [[CrossRef](#)] [[PubMed](#)]